Energy Dissipation in Driven Granular Matter in the Absence of Gravity

Achim Sack, Michael Heckel, Jonathan E. Kollmer, Fabian Zimber, and Thorsten Pöschel

Institut für Multiskalensimulation, Friedrich-Alexander-Universität Erlangen-Nürnberg, 91052 Erlangen, Germany

We experimentally investigate the energy dissipation rate in sinusoidally driven boxes which are partly filled by granular material under conditions of weightlessness. We identify two different modes of granular dynamics, depending on the amplitude of driving, A. For intense forcing, $A > A_0$, the material is found in the *collect-and-collide* regime where the center of mass of the granulate moves synchronously with the driven container, while for weak forcing, $A < A_0$, the granular material exhibits gaslike behavior. Both regimes correspond to different dissipation mechanisms, leading to different scaling with amplitude and frequency of the excitation and with the mass of the granulate. For the collect-and-collide regime, we explain the dependence on frequency and amplitude of the excitation by means of an effective one-particle model. For both regimes, the results may be collapsed to a single curve characterizing the physics of granular dampers.

When containers filled with granular material are subjected to vibrational motion, a number of interesting phenomena are observed. The most prominent among them are self-organized convection flows and various segregation effects which are reported in a large body of literature, e.g., [1–3]. Most, if not all, of these effects found in driven granular systems are influenced by gravity; therefore, to study these effects in the absence of gravity, experiments have been performed under conditions of weightlessness in parabolic flights, drop towers, and sounding rockets. Examples for such investigations concern shear flow [4], cooling and clustering in dilute systems [5–8], violations of the energy equipartition [9–11], the propagation of sound [12], and segregation [13].

In this Letter, we experimentally address the mechanisms of energy dissipation in vibrationally driven granular systems in the absence of gravity.

Dissipation mechanisms belong to the fundamental properties of matter and are of interest *per se*. But besides scientific curiosity, the investigation of dissipation in granular systems is of technological interest to dampen unwanted vibration by using devices referred to as *granular dampers* which are containers or cavities filled with granular material. When the container is subjected to oscillatory motion, the grains inside the cavity collide inelastically with one another and with the confinement and, thus, dissipate mechanical energy of the vibration. In contrast to conventional dashpot dampers, granular dampers do not rely on a fixed anchor as an impulse reservoir. They show only a minute dependence on temperature, and, since such dampers can be sealed off hermetically, they are predestined for long term use in harsh environments with extreme temperatures and/ or high pressures. For example, by using granular dampers, turbine blades can be kept from oscillating, and in medical tools where sterilization is mandatory they can dampen the vibration of handles [14–17].

Extensive research has been performed on understanding the behavior of granular dampers in specific applications and to determine the influence of material and construction parameters like the size of the container or cavity, the number of particles, the mass of the filling, and the clearance, e.g., [18–26]. Recent simulations show the flow of the granular material inside such a cavity under normal gravity for a vertically shaken system [24,25].

From all of these investigations it may be concluded that the dissipation properties of a granular damper depend in a nontrivial way on many variables like the amplitude of the oscillation, the clearance, and the frequency as well as the mass and type of particles [27,28]. By now, however, these dependencies are poorly understood.

Besides the lack of understanding the physics of such systems, from a technological point of view there is a need for a master design curve, in order to be able to *predict* the damping properties of a granular damper in a certain application.

As shown in the comprehensive work by Yang [21] for vertical excitation in gravity, only for strong forcing (high excitation energy) is it possible to collapse the dissipated power as a function of the amplitude for various frequencies and, thus, to deduce an empirical master design curve. For less intense driving it was shown by means of numerical simulations [29] that to a large extent the dissipative properties of granular dampers are influenced by gravity, in particular, when gravity exceeds the acceleration due to the external forcing.

To isolate the response of driven granular systems to external excitation from the disturbing effect of gravity, in this Letter for the first time we address the energy dissipation of granular dampers under conditions of weightlessness during parabolic flights. We explain the dependence on frequency and amplitude of the excitation by means of an effective one-particle model. Without using any
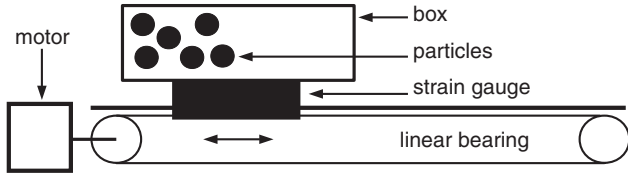
FIG. 1.   Sketch of the experiment. For an explanation, see the text.

adjustable parameter, the results may be collapsed to a single curve characterizing the physics of granular dampers.

Experiment.—The experimental setup is sketched in Fig. 1. The sample box is mounted on a strain gauge which in turn is attached to a carrier moving on a linear bearing. A gear belt connects the carrier with a computer controlled stepper motor which drives the carrier to perform sinusoidal oscillations of adjustable angular frequency ω and amplitude A. The time-dependent position of the container was measured by using Hall-effect-based position encoders with a resolution of 20 μm and a 10 kHz sample rate to check that the deviation of the container's motion from the set sinusoidal oscillation is negligibly small; typically, the spurious free dynamic range is 56 dB. The experiment was monitored by a high-speed camera at a frame rate of 240 fps. The entire setup was built up twice such that the containers move in opposite direction to cancel the vibrations transmitted to the external mounting structure.

The strain gauge delivered signals proportional to the forces in the direction of driving and the two directions perpendicular to it. Only the first one is relevant for our experiment; we checked that the forces in the other directions are negligibly small as compared to it; i.e., the side walls confine the granular material while the main transfer of momentum occurs parallel to the direction of motion.

The samples consist of polycarbonate boxes (wall thickness 4 mm) partially filled by different amounts of steel beads (diameter 4 mm, material density 7.8 g/cm^3, Young's modulus 203.5 GPa). The number and the total mass of particles within each sample is given by N and m, respectively. The clearance L_g is the difference between box length and the thickness of the packed layer of particles in the box. It can be obtained by computing the volume occupied by particles in random close packing [30] at

TABLE I.   Table of samples.

Sample no.	Box $L \times W \times H$ (mm^3)	m (g)	N	L_g (mm)
1	$100 \times 50 \times 50$	126.3	473	89.4
2	$50 \times 50 \times 50$	135.3	507	38.7
3	$50 \times 50 \times 50$	71.0	266	44.1
4	$100 \times 50 \times 50$	63.8	239	94.7

volume fraction 64%. Table I summarizes the characteristics of our samples.

To exclude the influence of gravity, the experiment was performed during a parabolic flight allowing for stable microgravity condition (0 ± 0.05) g for time intervals of about 22 s which determine the duration of each single measurement, where amplitude and frequency of the excitation were fixed. The data resulting from the strain gauges and the position sensors were sampled simultaneously at a rate of 10 kHz and stored for later evaluation of the dissipated energy. About 4 s after the onset of microgravity, the experiment had entered the stationary state which could be identified by both the rate of dissipation deduced from the measurement of the driving force and the recordings of the high-speed camera. For the results reported here, we use only the data obtained in the stationary state.

Regimes of dynamical behavior.—Analyzing the high-speed video recordings, we can identify two different regimes of dynamical behavior; see Fig. 2. For large amplitudes of the vibration, the damper operates in the collect-and-collide regime; that is, during the inward stroke all the material is "collected" and accumulates as a relatively densely packed layer at the wall of the container. After passing the phase of maximal velocity, the box decelerates and the layer of particles leaves the wall collectively. When the bulk of particles impacts the opposite wall of the container, a large part of the kinetic energy is dissipated by inelastic collisions. The amount of energy dissipated depends on the relative velocity between the

FIG. 2.   Snapshots from the high-speed video recordings of sample 4 illustrating the two distinct regimes of excitation: collect-and-collide regime at $A = 50$ mm (left column) and a gaslike state at $A = 2.5$ mm (right column). Each column shows the box at a phase range from 0 (top) to π (bottom).

particles and the wall at the time of the impact, determined by the amplitude and frequency of the vibration and the filling ratio of the container. The collect-and-collide regime was theoretically and experimentally investigated in Ref. [31] and identified as the regime of most efficient damping. It was confirmed also by numerical MD simulations [32,33] and identified as one out of four different regimes of dynamical behavior of vibrated granulate in microgravity.

For small amplitudes we observe a gaseous state where only a small fraction of the particles interact with the oscillating walls during one oscillation period. In the gaseous state, the collisions of the particles with the driving walls are just sufficient to balance the energy loss according to dissipative particle-particle collisions in the bulk of the material. Here, the dissipation rate is smaller than in the collect-and-collide regime [31].

Energy dissipation rate.—To obtain the energy dissipated by the granulate during one period, $T \equiv 2\pi/\omega$, of the sinusoidal driving, $x = A\sin(\omega t)$, we integrate the product of the measured force $F(t)$ and velocity $\dot{x}(t)$ over one period of oscillation:

$$E_{\text{diss}} \equiv \int_T \dot{x}(t)F(t)dt. \tag{1}$$

The maximum energy that can be dissipated during one cycle in the system is given by

$$E_{\text{max}} = 4mA^2\omega^2. \tag{2}$$

This is the case if all particles collide inelastically with the wall at maximum relative velocity. In the following, E_{max} is used for normalization.

We measured the dissipated energy per period for the following ranges of frequency: Samples 1 and 4 were shaken at 1, 2, and 4 Hz, while samples 2 and 3 were shaken from 1 to 5 Hz in 1 Hz increments. For each setup, Fig. 3 shows $E_{\text{diss}}/E_{\text{max}}$ versus the amplitude of the oscillation.

Let us first consider the gaslike state observed for small amplitude $A < A_0$. In this regime, we expect the dissipated energy to be proportional to the number of particles colliding with the wall. If we assume a monodisperse system with homogeneous density, this number is determined by the volume swept by the container's wall. We further assume the characteristic velocity of the particles to scale with the velocity of driving $A\omega$ and the particles hitting the wall at random phases, due to their disordered motion, and arrive at

$$E_{\text{diss}}^g \propto m \frac{A^3\omega^2}{L} = \frac{A}{4L}E_{\text{max}}. \tag{3}$$

Note that particle-particle collisions in the bulk of the material contribute only indirectly to E_{diss}^g, since such collisions do not transfer momentum to the container.
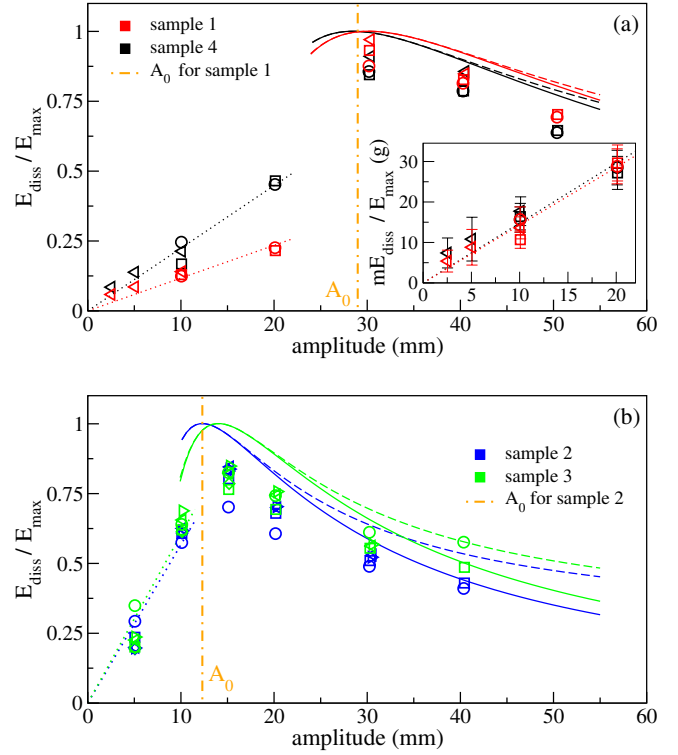

FIG. 3 (color online).   Normalized dissipated energy per period of external vibration. Symbols: Experimental data. ○: 1 Hz, □: 2 Hz, ◇: 3 Hz, ◁: 4 Hz; ▷: 5 Hz. Lines: Solution of the impact model, valid for $A > A_0$ [solid line, numerical, Eq. (6); dashed line, analytical, Eq. (9)]. Dotted lines: Dissipation rate for the gaseous regime [$A < A_0$; see Eq. (3)]. Inset: The same data (only gas regime) but normalized to E_{max}/m [see Eq. (4)]. The error bars for the gas regime are shown in the inset. For all other measurements, the errors are about the size of the symbols. The threshold amplitude A_0 (vertical lines) obtained from the model [see Eq. (10)] agrees with the experimental data.

Equation (3) was developed under the assumption of a homogenous density distribution. This, however, may not always hold true. Unlike molecular gases, heated granular gases are not homogeneous, but density increases in a nonlinear way with distance from the driving wall [34] to form regions of enhanced density (clusters) far away from the wall. Following the arguments of Ref. [35], the number of particle-wall collisions depends only weakly on the total mass of particles in the system. Consequently, for the limit of no dependence on the total mass we may write

$$\frac{E_{\text{diss}}^g}{E_{\text{max}}} \propto \frac{A}{4Lm}, \tag{4}$$

shown in the inset in Fig. 3(a).

For the cases described by Eqs. (3) and (4), the experimental data shown in Fig. 3 collapse despite the fact that the data points shown for a certain amplitude correspond to different frequencies of driving. That is, the dissipation rate

is independent of frequency in agreement with the scalings, Eq. (4) for Fig. 3(a) and Eq. (3) for Fig. 3(b).

For large amplitudes $A > A_0$, when the granulate is in the collect-and-collide regime, the experimental data collapse when scaled with E_{max}. Moreover, also here the scaled data belonging to the same amplitude are independent of the frequency. To quantitatively explain the data shown in Fig. 3 and to understand its independence of frequency for $A > A_0$, we take a closer look at the dynamics of the collect-and-collide regime, where nearly all particles are collected by the inward stroke and leave the wall collectively at $t = 0$ with velocity $v_{particle} = A\omega$. We define t_c as the time when the particles collide with the opposing wall where they will adopt its instantaneous velocity $v_{wall} = A\omega \cos(\omega t_c)$. Note that this corresponds to the motion of a quasiparticle interacting perfectly inelastically with the container walls. For a justification of this model, see [24,31,36]. The amount of kinetic energy lost per period depends on the difference of the velocity of the quasiparticle and the wall:

$$E_{diss}^{cc} = m(v_{particle} - v_{wall})^2. \tag{5}$$

Expressed in terms of t_c and E_{max} we obtain

$$E_{diss}^{cc} = \frac{1}{4}[1 - \cos(\omega t_c)]^2 E_{max}. \tag{6}$$

The time t_c is implicitly given by the distance the bulk of particles has traveled and the harmonic motion of the box:

$$v_{wall} t_c = A\omega t_c = A \sin(\omega t_c) + L_g. \tag{7}$$

Equation (7) can be solved numerically for ωt_c to obtain the dissipated energy per period, E_{diss}^{cc}/E_{max}, via Eq. (6) (see solid lines in Fig. 3).

Alternatively, we can obtain an approximate value for ωt_c by a first-order expansion of Eq. (7) around $\omega t_c = \pi$:

$$\omega t_c \approx \frac{\pi}{2} + \frac{L_g}{2A}. \tag{8}$$

Inserting this solution into Eq. (6), we find

$$\frac{E_{diss}^{cc}}{E_{max}} \approx \frac{1}{4}\left[1 - \sin\left(\frac{L_g}{2A}\right)\right]^2. \tag{9}$$

Figure 3 compares the relative dissipated energy per oscillation period as obtained in experiments (symbols) with the numerical solution of the collect-and-collide model, Eqs. (5) and (7), (solid lines) and its approximate analytical solution, Eq. (9) (dashed lines), resulting in good agreement. Also in agreement with the experimental data, both Eqs. (9) and (6) with ωt_c from Eq. (7) as well as Eqs. (3) and (4) are independent of the frequency ω, which explains the collapse of the data for different frequencies. Note that the model, Eqs. (6) and (7), and the approximate solution, Eq. (9), do not contain any adjustable parameters.

Furthermore, this model provides an explanation of the threshold A_0 separating the gaseous state from the collect-and-collide regime: The bulk of particles leaves the wall on its inward stroke at time $t = 0$ (instant of maximal velocity). If it arrives at the opposite wall at a time where the wall is accelerating away from it, that is, $\pi < \omega t_c < 2\pi$, it will not get collected by the wall but mainly scattered. This scattering inevitably leads to desynchronization of collective particle motion and the collect-and-collide mode breaks down. The threshold can be obtained from Eq. (8) with $\omega t_c = \pi$:

$$A_0 = \frac{L_g}{\pi}. \tag{10}$$

Interestingly, at the edge of stability of the collect-and-collide regime, $A = A_0$, that is, $\omega t_c = \pi$, from Eq. (6) we obtain maximal efficiency in damping. The threshold amplitude A_0 obtained from the model agrees well with the experimental data; see Fig. 3 (vertical lines).

Conclusion.—On Earth, the influence of gravity on granular dynamics can be neglected only for intense driving, where $A\omega^2 \gg g$. To study the response of granular dampers to external excitation isolated from the disturbing effect of gravity, we investigated the energy dissipation of granular matter in the absence of gravity when subjected to sinusoidal motion, $x(t) = A \sin(\omega t)$.

Depending on the amplitude of the vibration, we observe two qualitatively different modes: For small amplitude $A < A_0 \approx L_g/\pi$, the granular material behaves gaslike, while for larger amplitudes $A > A_0$, we observe a collect-and-collide regime where the center of mass of the granulate moves synchronously with the driven container. In this regime, we describe the system by an effective one-particle model, Eq. (6), which can be solved numerically or by using an analytical approximation. Despite the model's simplicity, we find remarkably good agreement with the experimental data.

In the gas regime, the energy dissipation rate increases linearly with the amplitude A. For large clearance L_g, the energy dissipation rate is almost independent of the mass of the granulate in agreement with the known density instability in granular gases, Eq. (4). Here an addition of particles hardly increases the density in the vicinity of the heated wall [35]. For smaller clearance, the high-density region is no longer far away from the driving wall such that the energy dissipation rate increases linearly with the mass, Eq. (4).

In both regimes, gaslike and collect-and-collide, the energy dissipation rate was found independent of the frequency, in agreement with our model description, Eqs. (3), (4), and (6).

With appropriate scaling, for a fixed container geometry all measurements coincide along one universal "master curve," independent of filling fraction, mass of the granulate, particle properties, particle number, and the parameters of vibration. Based on the theory of granular gases for the gas state and on the effective one-particle model for the

[1] J. B. Knight, H. M. Jaeger, and S. R. Nagel, Phys. Rev. Lett. **70,** 3728 (1993).

[2] J. A. C. Gallas, H. J. Herrmann, and S. Sokołowski, Phys. Rev. Lett. **69,** 1371 (1992).

[3] I. Aranson and L. Tsimring, *Granular Patterns* (Oxford University Press, Oxford, 2009).

[4] N. Murdoch, B. Rozitis, K. Nordstrom, S. F. Green, P. Michel, T.-L. de Lophem, and W. Losert, Phys. Rev. Lett. **110,** 018307 (2013).

[5] E. Falcon, R. Wunenburger, P. Évesque, S. Fauve, C. Chabot, Y. Garrabos, and D. Beysens, Phys. Rev. Lett. **83,** 440 (1999).

[6] S. Tatsumi, Y. Murayama, H. Hayakawa, and M. Sanoi, J. Fluid Mech. **641,** 521 (2009).

[7] Y. Grasselli, G. Bossis, and G. Goutallier, Europhys. Lett. **86,** 60007 (2009).

[8] K. Harth, U. Kornek, T. Trittel, U. Strachauer, S. Höme, K. Will, and R. Stannarius, Phys. Rev. Lett. **110,** 144102 (2013).

[9] Y. P. Chen, P. Evesque, and M.-Y. Hou, Chin. Phys. Lett. **29,** 074501 (2012).

[10] M. Hou, R. Liu, G. Zhai, Z. Sun, K. Lu, Y. Garrabos, and P. Evesque, Microgravity Sci. Technol. **20,** 73 (2008).

[11] M. Leconte, Y. Garrabos, E. Falcon, C. Lecoutre-Chabot, F. Palencia, P. Evesque, and D. Beysens, J. Stat. Mech. (2006) P07012.

[12] X. Zeng, J. H. Agui, and M. Nakagawa, J. Aerosp. Eng. **20,** 116 (2007).

[13] C. Güttler, I. von Borstel, R. Schräpler, and J. Blum, Phys. Rev. E **87,** 044201 (2013).

[14] R. Kielb, F. Macri, D. Oeth, A. Nashif, P. Macioce, H. Panossian, and F. Lieghley, in Proceedings of the 4th National Turbine Engine High Cycle Fatigue Conference, Monterey, CA, 1999.

[15] M. Heckel, A. Sack, J. E. Kollmer, and T. Pöschel, Physica (Amsterdam) **391A,** 4442 (2012).

[16] J. Norcross, U.S. Patent, No. 3343576 (1967).

[17] Z. Xia, X. Liu, and Y. Shan, Int. J. Veh. Noise Vib. **7,** 178 (2011).

[18] M. Sadek and B. Mills, J. Mech. Eng. Sci. **12,** 268 (1970).

[19] M. Sadek and C. Williams, J. Mech. Eng. Sci. **12,** 278 (1970).

[20] C. Salueña, T. Pöschel, and S. E. Esipov, Phys. Rev. E **59,** 4422 (1999).

[21] M. Y. Yang, Ph.D. thesis, Pennsylvania State University, 2003.

[22] X.-M. Bai, L. M. Keer, Q. J. Wang, and R. Q. Snurr, Granular Matter **11,** 417 (2009).

[23] M. Sánchez and L. A. Pugnaloni, J. Sound Vib. **330,** 5812 (2011).

[24] M. Sánchez, G. Rosenthal, and L. A. Pugnaloni, J. Sound Vib. **331,** 4389 (2012).

[25] M. Sánchez and C. M. Carlevaro, J. Sound Vib. **332,** 2070 (2013).

[26] Z. Cui, J. H. Wu, H. Chen, and D. Li, J. Sound Vib. **330,** 2449 (2011).

[27] K. S. Marhadi and V. K. Kinra, J. Sound Vib. **283,** 433 (2005).

[28] A. Ham, J. Wang, and J. G. Stammer, J. Geotech. Geoenviron. Eng. **138,** 1002 (2012).

[29] C. Salueña, S. Esipov, T. Pöschel, and S. Simonian, Proc. SPIE Int. Soc. Opt. Eng. **3327,** 23 (1998).

[30] T. Aste and D. L. Weaire, *The Pursuit of Perfect Packing* (Institute of Physics, Bristol, 2000).

[31] M. N. Bannerman, J. E. Kollmer, A. Sack, M. Heckel, P. Mueller, and T. Pöschel, Phys. Rev. E **84,** 011301 (2011).

[32] E. Opsomer, F. Ludewig, and N. Vandewalle, Phys. Rev. E **84,** 051306 (2011).

[33] E. Opsomer, F. Ludewig, and N. Vandewalle, J. Phys. Conf. Ser. **327,** 012035 (2011).

[34] E. L. Grossman, T. Zhou, and E. Ben-Naim, Phys. Rev. E **55,** 4200 (1997).

[35] B. Meerson, T. Pöschel, P. V. Sasorov, and T. Schwager, Phys. Rev. E **69,** 021302 (2004).

[36] S. Luding, Ph.D. thesis, Universität Freiburg, 1994, http://www2.msm.ctw.utwente.nl/sluding/PAPERS/PhD_Luding.pdf.